CHEMISTRY
A EUROPEAN JOURNAL

DOI: 10.1002/chem.200801139

Head-to-Head Right-Handed Cross-Links of the Antitumor-Active Bis(μ-*N,N′*-di-*p*-tolylformamidinato)dirhodium(II,II) Unit with the Dinucleotides d(GpA) and d(ApG)

Helen T. Chifotides* and Kim R. Dunbar*[a]

Dedicated to Professor Jan Reedijk on the occasion of his 65th birthday and retirement

Abstract: Reactions of *cis*-[Rh_2-(DTolF)$_2$($NCCH_3$)$_6$](BF_4)$_2$ with the dinucleotides d(GpA) and d(ApG) proceed to form [Rh_2(DTolF)$_2${d(GpA)}] and [Rh_2(DTolF)$_2${d(ApG)}], respectively, with bridging purine bases spanning the Rh–Rh unit in the equatorial positions. Both dirhodium adducts exhibit head-to-head (HH) arrangement of the bases, as indicated by the presence of H8/H8 NOE cross-peaks in the 2D ROESY NMR spectra. The guanine bases bind to the dirhodium core at positions N7 and O6, a conclusion that is supported by the absence of N7 protonation at low pH values and the notable increase in the acidity of the guanine N1H sites (pK_a≈7.4 in 4:1 CD_3CN/D_2O), inferred from the pH-dependence titrations of the guanine H8 proton resonances. In both dirhodium adducts, the adenine bases coordinate to the metal atoms through N6 and N7, which induces stabilization of the rare imino tautomer of the bases with a concomitant substantial decrease in the basicity of the N1H adenine sites (pK_a≈7.0–7.1 in 4:1 CD_3CN/D_2O), as compared to the imino form of free adenosine. The presence of the adenine bases in the rare imino form is further corroborated by the observation of DQF-COSY H2/N1H and ROE N1H/N6H cross-peaks in the 2D NMR spectra of [Rh_2(DTolF)$_2${d(GpA)}] and [Rh_2(DTolF)$_2${d(ApG)}] in CD_3CN at −38 °C. The 2D NMR spectroscopic data and the molecular modeling results suggest the presence of right-handed variants, HH1R, in solution for both adducts (HH1R refers to the relative base canting and the direction of propagation of the phosphodiester backbone with respect to the 5′ base). Complete characterization of [Rh_2(DTolF)$_2${d(GpA)}] and [Rh_2(DTolF)$_2${d(ApG)}] by 2D NMR spectroscopy and molecular modeling supports *anti*-orientation of the sugar residues for both adducts about the glycosyl bonds as well as N- and S-type conformations for the 5′- and 3′-deoxyribose residues, respectively.

Keywords: antitumor agents · bioinorganic chemistry · formamidinates · nucleic acids · rhodium

Introduction

Metal–metal bonded dirhodium carboxylate bioinorganic compounds with a lantern-type structure[1] are interesting targets for research because of their considerable carcinostatic activity against various tumor cell lines,[2–9] their unusual binding modes to DNA,[10–15] and their documented inhibition of DNA replication, protein synthesis, and in vitro transcription.[16–18] A closely related class of dirhodium compounds to the tetracarboxylate series is one in which two acetate ligands are substituted by the more robust amidinate groups. Of particular note is the compound *cis*-[Rh_2-(DTolF)$_2$(O_2CCF_3)$_2$(H_2O)$_2$] (DTolF$^-$ = *N,N′*-di-*p*-tolylformamidinate; Scheme 1), which exhibits comparable antitumor activity to that of dirhodium carboxylate compounds and cisplatin against Yoshida ascites and T8 sarcomas, but with considerably reduced toxicity.[19] Despite the presence of two labile trifluoroacetate bridging groups, which impart appreciable reactivity to the complex, *cis*-[Rh_2(DTolF)$_2$-(O_2CCF_3)$_2$(H_2O)$_2$] was found to be virtually nontoxic.[19]

Reactions of dirhodium compounds with purine nucleobases,[13,20,21] nucleosides/nucleotides,[22–25] single-[10,11] and double-stranded DNA[12,15] have received considerable attention in light of DNA being the primary intracellular

[a] Dr. H. T. Chifotides, Prof. K. R. Dunbar
Department of Chemistry, Texas A&M University
College Station, TX 77843 (USA)
Fax: (+1) 979-845-7177
E-mail: chifotides@mail.chem.tamu.edu
dunbar@mail.chem.tamu.edu

Supporting Information for this article is available on the WWW under http://dx.doi.org/10.1002/chem.200801139.

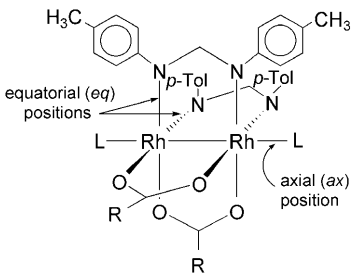

Scheme 1. Structure of *cis*-$[Rh_2(DTolF)_2(O_2CCF_3)_2L_2]$; $R = CF_3$.

target of most metal-based anticancer agents. It is well-established that 1,2-GG and AG intrastrand cross-links account for about 65% and 25%, respectively, of the DNA-binding sites for cisplatin (a widely used anticancer agent),[26–29] with 5′-G sites of 5′-GG-3′ cross-links being the most electron-donating sites in B DNA.[30] In the case of dirhodium, findings in our laboratories have unequivocally established that guanine bases bind to the metal core in a manner involving unprecedented equatorial (*eq*) bridging interactions through N7 and O6.[13] Head-to-head (HH)[31a] cross-links with *eq* bidentate (N7/O6) guanine bases bridging the Rh–Rh bond were also identified in the dinucleotide dirhodium adducts $[Rh_2(O_2CCH_3)_2\{d(GpG)\}]$,[22] $[Rh_2(O_2CCH_3)_2\{d(pGpG)\}]$,[23] and $[Rh_2(DTolF)_2\{d(GpG)\}]$.[24] Notable features of the adducts are the deprotonation of the guanine N1 site, that is, stabilization of the enolate form of guanine, and a substantial increase in the acidity of the N1H sites as a result of bidentate N7/O6 coordination.[13,22–24] In the aforementioned d((p)GpG) complexes, the presence of intense H8/H8 ROE (rotating frame nuclear Overhauser effect) cross-peaks in the 2D ROESY NMR spectra indicate a HH arrangement for the tethered guanine bases. The $[Rh_2(O_2CCH_3)_2\{d(GpG)\}]$ complex exhibits two major right-handed conformers HH1R (≈75%) and HH2R (≈25%),[22] as opposed to only one right-handed HH1R conformer for $[Rh_2(DTolF)_2\{d(GpG)\}]$.[24] In the latter case, the detection of a single product is attributed to the presence of the bulky, nonlabile formamidinate bridging groups, which serve to slow down the possible dynamic processes for the adduct[32] that would lead to the formation of the minor HH2R variant detected for the acetate.[22] The terms HH1R and HH2R, initially proposed for platinum compounds by Kozelka et al.,[33,34] and refined by Marzilli, Natile et al.,[32,35–39] refer to the relative base canting[31b] and the direction of propagation of the phosphodiester backbone with respect to the 5′ base.[22,24]

Dirhodium axial adducts with adenine derivatives and carboxylate bridging groups exhibit hydrogen bonds between the purine exocyclic $NH_2(6)$ amino group (the base is coordinated by N7) and the carboxylate oxygen atom of the dirhodium unit.[13] The reaction of *cis*-$[Rh_2(DTolF)_2(NCCH_3)_6](BF_4)_2$ with 9-ethyladenine (9-EtAdeH), however, proceeds by substitution of the acetonitrile groups and affords HT *cis*-$[Rh_2(DTolF)_2(9\text{-}EtAdeH)_2(NCCH_3)](BF_4)_2$ with the adenine bases bridging through N7 and N6 at the *eq* sites of the two rhodium atoms.[40,41] This unprecedented adenine-bridging binding mode is also encountered in the dinucleotide adduct $[Rh_2(DTolF)_2\{d(ApA)\}]$.[25] In the right-handed HH1R dirhodium conformer of this adduct, the tethered adenine bases exhibit a HH arrangement and are found in the rare imino form, exhibiting a concomitant substantial decrease in the basicity of the N1H sites ($pK_a \approx 7.0$ in CD_3CN/D_2O) as compared to the imino form of the free dinucleotide; this decrease is a result of coordination of the N7/N6 adenine sites to the rhodium atoms.[25] In DNA, adenine is mainly present as its amine tautomer,[42,43] which is estimated to outnumber the rare imino form A* by a factor of 10^4–10^5. Metal binding to the exocyclic amino group N6, however, may be accompanied by a concomitant shift of the amino proton to site N1, thus generating a metalated form of the rare adenine imino tautomer.[25,44–49]

The unprecedented binding modes and conformational characteristics encountered in the homopurine adducts $[Rh_2(DTolF)_2\{d(GpG)\}]$[24] and $[Rh_2(DTolF)_2\{d(ApA)\}]$[25] led us to undertake structural characterization of the mixed purine complexes $[Rh_2(DTolF)_2\{d(GpA)\}]$ and $[Rh_2(DTolF)_2\{d(ApG)\}]$ by one- (1D) and two-dimensional (2D) NMR spectroscopy, combined with molecular modeling studies. Moreover, the 1,2-ApG cross-links have been extensively studied,[50–52] as they are the next most abundant intrastrand adducts found for cisplatin (after the 1,2-GpG) that are recognized by the HMG proteins.[53] For cisplatin, GpA cross-links have been detected with d(GpA) dinucleotides[54,55] but not with double-stranded DNA.[51,52] In the case of dirhodium compounds bridged by carboxylate groups, single-stranded DNA oligonucleotides containing mixed AG and GA purine sites have been studied by mass spectrometry,[11] but to our knowledge, herein is the first detailed NMR study of the products between the mixed-purine DNA dinucleotides d(GpA) or d(ApG) (Scheme 2) and a metal–metal-bonded dirhodium formamidinate unit.

Results

1D ^{1}H NMR spectroscopy: In the ^{1}H NMR spectrum for each of the dirhodium adducts $[Rh_2(DTolF)_2\{d(GpA)\}]$ and $[Rh_2(DTolF)_2\{d(ApG)\}]$, there is a triplet at $\delta \approx 7.45$ ppm (with twice the intensity of each purine H8 or H2 resonance), which is ascribed to the two N-C*H*-N proton nuclei of the two bridging formamidinate groups for each adduct (the splittings are attributed to ^{1}H coupling to the two equivalent rhodium nuclei, $^3J\{^{103}Rh–^1H\} \approx 3.9$ Hz). For *cis*-$[Rh_2(DTolF)_2(NCCH_3)_6](BF_4)_2$, δ(N-C*H*-N) = 7.51 ppm in CD_3CN.[24]

$[Rh_2(DTolF)_2\{d(GpA)\}]$: In the aromatic region of the ^{1}H NMR spectrum for the dirhodium adduct in 4:1 CD_3CN/D_2O at 20°C, the two resonances at $\delta = 8.62$ and 7.96 ppm are assigned to the 5′-G and 3′-A H8 protons, respectively (Table 1) by analysis of 2D NMR spectroscopic data (vide infra); the aromatic resonance at $\delta = 7.81$ ppm is attributed

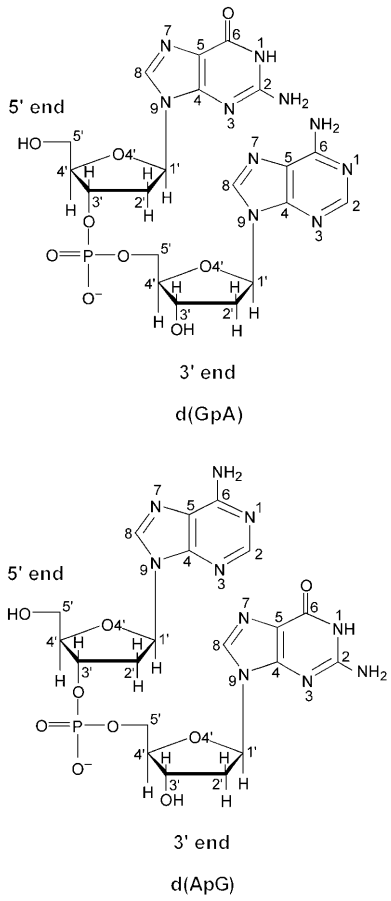

Scheme 2. Structure and atom numbering of the dinucleotides d(GpA) and d(ApG).

to the 3′-A H2 proton, an assignment also confirmed by its longer T_1 relaxation time as compared to H8.[56–58] Although the NMR data for $[Rh_2(DTolF)_2\{d(GpA)\}]$ and d(GpA) were collected in different solvents (the complex is not soluble in D_2O only), a comparison of the aromatic proton chemical shifts is still useful: the resonance of 5′-G H8 is shifted downfield ($\Delta\delta \approx 1$ ppm), whereas the 3′-A H8 and H2 protons are shifted upfield by $\Delta\delta \approx 0.40$ and 0.13 ppm, respectively, as compared to the corresponding protons in free d(GpA). Similar changes to the chemical shifts of the aromatic proton resonances of metalated adenine rings have been previously recorded in the literature.[47,48] Additionally, downfield shifts of the guanine H8 proton indicate metal binding to site N7 of the base.[22,23,59]

$[Rh_2(DTolF)_2\{d(ApG)\}]$: In a similar fashion to $[Rh_2(DTolF)_2\{d(GpA)\}]$, the two aromatic resonances in the ^{1}H NMR spectrum of $[Rh_2(DTolF)_2\{d(ApG)\}]$ in 4:1 CD_3CN/D_2O (at 20 °C) at $\delta = 8.74$ and 7.70 ppm are assigned to the 5′-A and 3′-G H8 protons, respectively (Table 1) by analysis of 2D NMR spectroscopic data (see below). The aromatic resonance at $\delta = 7.62$ ppm is assigned to the 5′-A H2 proton, an assignment also confirmed by its longer T_1 relaxation time as compared to H8.[56–58] Although the H8 protons of purine bases metalated at N7 are typically shifted downfield as compared to the free base, the 3′-G H8 of $[Rh_2(DTolF)_2\{d(ApG)\}]$ exhibits an upfield shift as compared to the free dinucleotide, which is attributed to the relative canting of the bases.[24,37]

pH-dependence titrations for dirhodium adducts: Since it is known that protonation and metalation of the in-ring nitrogen atoms of purine nucleobases have profound effects on the chemical shifts of the H8 aromatic protons,[60] ^{1}H NMR titrations as a function of pH were performed in 4:1 CD_3CN/D_2O for $[Rh_2(DTolF)_2\{d(GpA)\}]$ (Figure 1) and $[Rh_2(DTolF)_2\{d(ApG)\}]$ (Figure 2). The pH-independent behavior of the H8 ^{1}H NMR signals at low pH corroborates

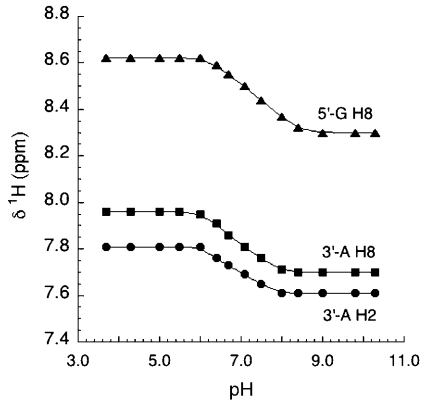

Figure 1. pH dependence of the 5′-G H8 (▲), 3′-A H8 (■), 3′-A H2 (●) ^{1}H NMR signals for $[Rh_2(DTolF)_2\{d(GpA)\}]$ in 4:1 CD_3CN/D_2O at 20 °C.

Table 1. ^{1}H and ^{31}P NMR chemical shifts, δ [ppm] for $[Rh_2(DTolF)_2\{d(GpA)\}]$ and $[Rh_2(DTolF)_2\{d(ApG)\}]$.

d(BpB) species	B	H8	H2	H1′	$^3J_{H1'-H2'}/^3J_{H1'-H2''}$[c]	H2′	H2″	H3′	H4′	H5′/H5″	N1H/N6H[f]	Base sugar	^{31}P[g]
$[Rh_2(DTolF)_2\{d(GpA)\}]$[a]	5′	8.62	–	6.11	0/10.0(d)	2.11	2.58	4.75	3.93	3.84[d]		*anti*	−3.16
	3′	7.96	7.81	6.28	14.2/6.0(dd)	2.38	2.44	4.48	4.02	3.95/3.77[e]	10.32/6.98	*anti*	
d(GpA)[b]	5′	7.72	–	5.86		2.09	2.30	4.75	4.18	4.15[d]		*anti*	−4.06
	3′	8.36	7.94	6.35		2.55	2.82	4.80	4.23	4.12[d]		*anti*	
$[Rh_2(DTolF)_2\{d(ApG)\}]$[a]	5′	8.74	7.62	6.14	0/7.0(d)	2.20	2.38	4.68	3.98	3.81[d]	7.29/7.10	*anti*	−2.29
	3′	7.70	–	6.16	13.0/5.0(dd)	2.28	2.60	4.74	3.89	3.70[d]		*anti*	
d(ApG)[b]	5′	7.91	7.97	5.94		2.41	2.70	4.73	4.16	4.12/4.08[e]		*anti*	−4.09
	3′	7.99	–	6.10		2.20	2.50	4.75	4.19	3.68[d]		*anti*	

[a] 2D NMR spectra collected in 4:1 CD_3CN/D_2O at 10 °C. [b] 2D NMR spectra collected in D_2O at 5 °C. [c] In Hertz. [d] Overlapped resonances. [e] Not stereospecifically assigned. [f] Chemical shifts at −38 °C. [g] Referenced to TMP at 0 ppm.

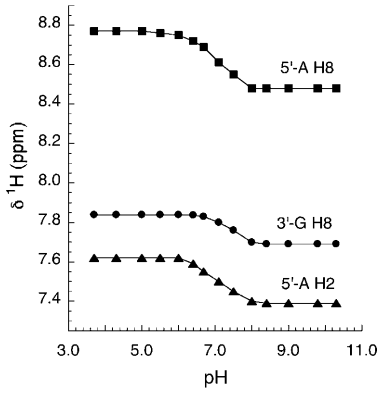

Figure 2. pH dependence of the 5′-A H8 (■), 5′-A H2 (▲), 3′-G H8 (●) ^{1}H NMR signals for $[Rh_2(DTolF)_2\{d(ApG)\}]$ in 4:1 CD_3CN/D_2O at 20 °C.

the binding of the guanine bases to the dirhodium units through N7 in both adducts (as protonation of these sites is impeded by bound metal atoms). Moreover, inflection points are observed for the 5′-G and 3′-G H8 protons of $[Rh_2(DTolF)_2\{d(GpA)\}]$ and $[Rh_2(DTolF)_2\{d(ApG)\}]$, respectively, at p$K_a \approx 7.4$, which correspond to deprotonation of the N1 sites of the two guanine bases. For free d(GpG) the pK_a value for N1H deprotonation is ~10.0 in D_2O;[22] the pK_a value of N1H deprotonation in CD_3CN, however, has been estimated to be higher than 10.0 (owing to the insolubility of d(GpA) and d(ApG) in CH_3CN, it is not possible to perform a pH-dependence titration of their guanine aromatic protons in CD_3CN).[61–63] The substantial decrease in the pK_a values of the guanine N1H groups in $[Rh_2(DTolF)_2\{d(GpA)\}]$ and $[Rh_2(DTolF)_2\{d(ApG)\}]$ (p$K_a \approx 7.4$), as compared to the guanine bases in the free dinucleotides, is attributed to bidentate binding of the guanine bases to the dirhodium units through N7 and O6 (Scheme 4).[22,24]

Regarding the adenine bases, protonation of the common amino tautomer of adenine (Scheme 3a) at N1 in H_2O takes place at p$K_a \approx 3$–4 (which decreases to ~2 upon metal binding to N7).[64–65,67] Protonation of the adenine N7 position takes place below pH 0,[68] whereas the exocyclic group N6H is deprotonated at pK_a 16.7.[69] In the case of the rare imino form of (methyl)adenine (Scheme 3b), however, the pK_a value for N1H deprotonation in H_2O has been estimated to be ~12.[70] Moreover, the expected pK_a value for deprotonation of the exocyclic groups N6H of deoxyadenosine is approximately 16, as a result of the inductive effect of the (deoxy)ribose group;[71–73] the estimated pK_a value for N1H deprotonation for the imino form of deoxyadenosine in H_2O is ~11.[70] It is thus inferred that the estimated pK_a values for N1H deprotonation for the imino form of adenosine in d(GpA) and d(ApG) in CD_3CN/D_2O should be much higher than 11.[61,62] The inflection points from the pH-dependence curves of the 3′-A and 5′-A H2 and H8 ^{1}H NMR signals for $[Rh_2(DTolF)_2\{d(GpA)\}]$ (Figure 1) and $[Rh_2(DTolF)_2\{d(ApG)\}]$ (Figure 2) in 4:1 CD_3CN/D_2O at 20 °C, respectively, at p$K_a \approx 7.0$ and 7.1, correspond to deprotonation of the N1H groups of the adenine bases in the rare imino form. Evidently, the pK_a values of the adenine exocyclic N6H sites in $[Rh_2(DTolF)_2\{d(GpA)\}]$ and $[Rh_2(DTolF)_2\{d(ApG)\}]$ are considerably decreased as compared to the imino form of the adenine bases in d(GpA) and d(ApG) in the same solvent. The substantial decrease in the basicity of the adenine N1H groups in both of the bis-formamidinate dinucleotide adducts is attributed to the presence of the adenine bases in the rare imino form, which is stabilized by the binding of N7 and N6 to the dirhodium unit (Scheme 4).[25,47,49]

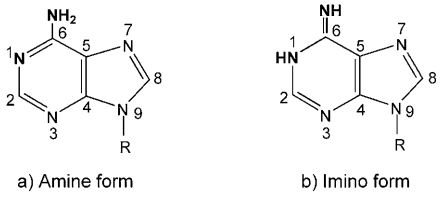

Scheme 3. Amine and imino tautomeric forms of adenine.

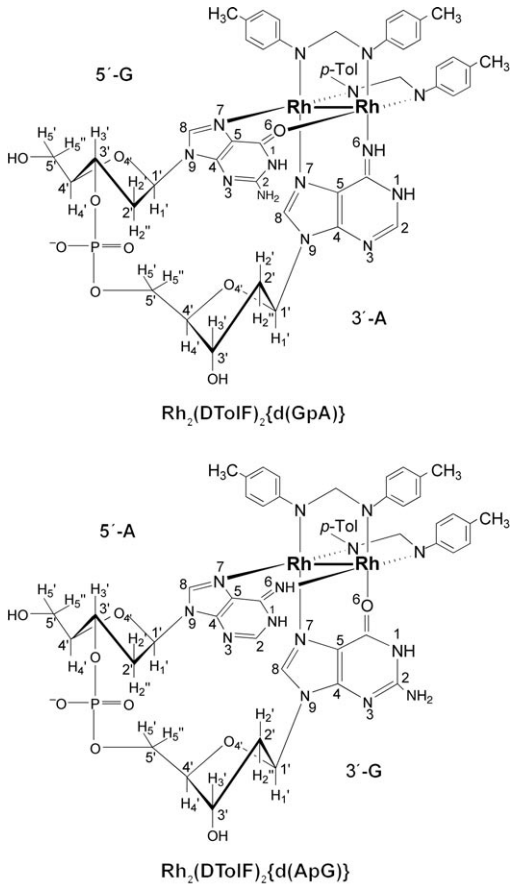

Scheme 4. Structure and numbering of $[Rh_2(DTolF)_2\{d(GpA)\}]$ (top panel) and $[Rh_2(DTolF)_2\{d(ApG)\}]$ (bottom panel). Note that bond lengths are not to scale and that angles between atoms have been distorted to render the structures more clear. Both A and G nucleotides are depicted in their neutral forms in the complexes (imino form for A, ketone form for G) because they have essentially identical pK_a values for N1 deprotonation when bound to the dirhodium core (see text).

2D NMR spectroscopy: 2D ROESY, [^{1}H–^{1}H] DQF-COSY (double-quantum-filtered correlation spectroscopy) and [^{1}H–^{31}P] HETCOR (heteronuclear shift correlation) NMR spectra were collected to assess the structural features and assign the proton resonances of the [Rh_2(DTolF)$_2${d(GpA)}] and [Rh_2(DTolF)$_2${d(ApG)}] adducts (Table 1).

[Rh_2(DTolF)$_2${d(GpA)}]: In the aromatic region of the 2D ROESY NMR spectrum of [Rh_2(DTolF)$_2${d(GpA)}], the two H8 resonances at $\delta = 8.62$ and 7.96 ppm are well separated and exhibit intense 5′-G H8/3′-A H8 NOE (nuclear Overhauser effect) cross-peaks (Figure 3, upper panel), features that are consistent with HH base orientation (Scheme 4) as previously reported for dirhodium d(GpG)[22–24] and d(ApA)[25] as well as platinum d(GpG) compounds.[32,35–37] Head-to-tail (HT) conformers do not exhibit H8/H8 cross-peaks as a result of large H8–H8 distances.[32,35–37] The downfield H8 resonance at $\delta = 8.62$ ppm is unambiguously assigned to 5′-G because it exhibits a strong H8/H3′ cross-peak in the 2D ROESY spectrum; moreover, this H3′ proton ($\delta = 4.75$ ppm) displays a cross-peak in the [^{1}H–^{31}P] HETCOR spectrum to the phosphodiester ^{31}P NMR signal at $\delta = -3.16$ ppm, whereas H5′/H5″–^{31}P and H4′–^{31}P cross-peaks are observed for 3′-A only (Figure 4). In the 300 ms 2D ROESY NMR spectrum, the H3′ proton of 5′-G ($\delta = 4.75$ ppm) has a much weaker cross-peak (in comparison to the intraresidue peak at $\delta = 8.62$ ppm) to a resonance in the aromatic region at $\delta = 7.96$ ppm, which is assigned to H8 of 3′-A.

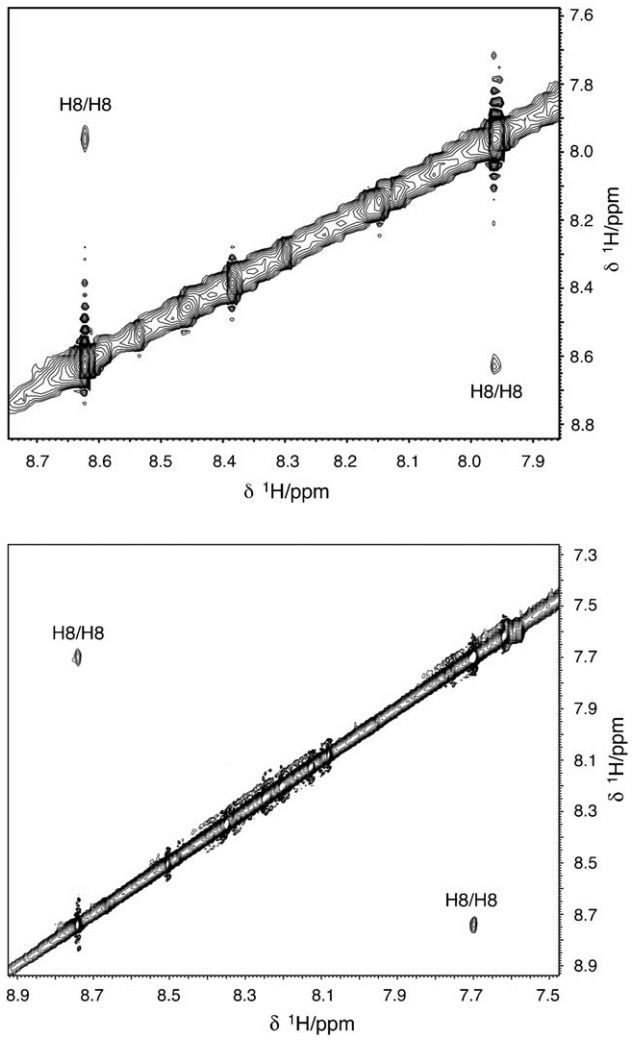

Figure 3. Aromatic regions of the 2D ROESY NMR spectra for [Rh_2(DTolF)$_2${d(GpA)}] (upper panel) and [Rh_2(DTolF)$_2${d(ApG)}] (lower panel) in 4:1 CD_3CN/D_2O at 10 °C, with labeled H8/H8 base cross-peaks.

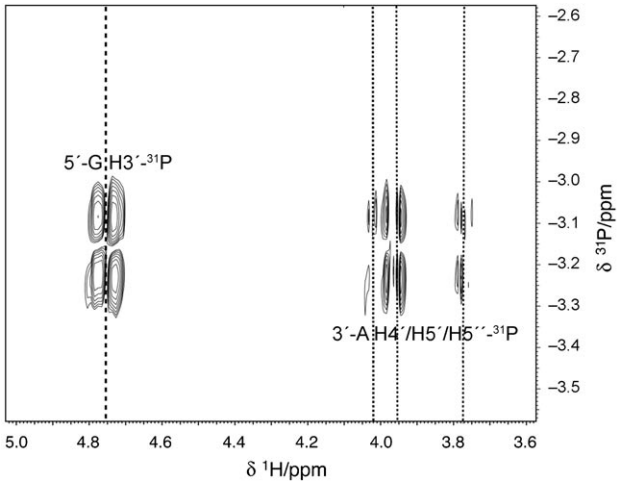

Figure 4. [^{1}H–^{31}P] HETCOR NMR spectrum for [Rh_2(DTolF)$_2${d(GpA)}] in 4:1 CD_3CN/D_2O at 10 °C. The dashed and dotted lines indicate the 5′-G and 3′-A deoxyribose proton resonances, respectively.

Both nucleotide residues in [Rh_2(DTolF)$_2${d(GpA)}] exhibit strong H8/H2′/H2″ ROE cross-peaks and the sugar rings have very weak (for 5′-G) or lack H8/H1′ ROE cross-peaks, which are features consistent with *anti* glycosidic torsion angles.[22–25,35–37,74] Furthermore, the 5′-G residue exhibits a strong H8/H3′ ROE cross-peak along with H1′-H2″ (no H1′–H2′ coupling; $^3J_{H1'-H2'} = 0$, Table 1) DQF-COSY cross-peaks and a doublet coupling pattern for its H1′ in the [^{1}H–^{1}H] DQF-COSY spectrum; these findings are characteristic of an C3′–endo (N-type) deoxyribose conformation for 5′-G.[22–25,35–37,74,75] Conversely, the 3′-A sugar retains the S (C2′–endo) conformation found in standard B-DNA, which is indicated by the appearance of a strong H1′–H2′ DQF COSY cross-peak along with the doublet of doublets coupling pattern observed for the H1′ resonance.[22,23,25,35–37,74,75]

[Rh_2(DTolF)$_2${d(ApG)}]: As noted for the H8 aromatic resonances of [Rh_2(DTolF)$_2${d(GpA)}], the two H8 resonances for [Rh_2(DTolF)$_2${d(ApG)}] at $\delta = 8.74$ and 7.70 ppm are well separated (~1 ppm) and exhibit intense 5′-A H8/3′-G H8 NOE cross-peaks in the aromatic region of the 2D ROESY NMR spectrum (Figure 3, lower panel), which indicates HH base orientation (Scheme 4), as previously reported for

dirhodium d(GpG)[22–24] and d(ApA)[25] as well as platinum d(GpG)[32,35–37] compounds. The downfield H8 resonance at $\delta = 8.74$ ppm is assigned to 5′-A as indicated by the strong H8/H3′ cross-peak that it exhibits in the 2D ROESY spectrum. This H3′ proton ($\delta = 4.68$ ppm) has a cross-peak in the [^{1}H–^{31}P] HETCOR spectrum to the phosphodiester ^{31}P NMR signal ($\delta = -2.29$ ppm), whereas H5′/H5″–^{31}P and H4′–^{31}P cross-peaks are observed for 3′-G only. In the 150 ms 2D ROESY NMR spectrum of [Rh_2(DTolF)$_2$-{d(ApG)}], the H3′ proton of 5′-A ($\delta = 4.68$ ppm) has a much weaker cross-peak (as compared to the intraresidue peak at $\delta = 8.74$ ppm) to a resonance in the aromatic region at $\delta = 7.70$ ppm, which is assigned to the H8 of 3′-G. Both nucleotide residues in [Rh_2(DTolF)$_2${d(ApG)}] show medium intensity H8/H2′ and very weak H8/H1′ ROE cross-peaks, which indicate *anti* glycosidic torsion angles.[22–25,35–37,74] Moreover, the 5′-A residue exhibits a strong H8/H3′ ROE cross-peak, no H1′–H2′ DQF-COSY cross-peaks ($^3J_{H1'-H2'} = 0$, Table 1) and a doublet coupling pattern for its H1′ in the [^{1}H–^{1}H] DQF-COSY spectrum, in contrast to the 3′-G sugar which has a strong H1′–H2′ DQF COSY cross-peak and a doublet of doublets coupling pattern for the H1′ resonance. These findings indicate C3′–endo (N-type) and S (C2′–endo) deoxyribose conformations for the 5′-A and 3′-G sugar residues, respectively.[22–25,35–37,74,75]

Imino form of the adenine bases: The presence of the adenine rings of [Rh_2(DTolF)$_2${d(GpA)}] and [Rh_2(DTolF)$_2${d-(ApG)}] in the rare imino form was confirmed by [^{1}H–^{1}H] DQF-COSY spectroscopy experiments performed at −38 °C.[25,47] In the low-field region of the [^{1}H–^{1}H] DQF-COSY spectrum for [Rh_2(DTolF)$_2${d(GpA)}] in CD_3CN at −38 °C, cross-peaks are observed between the H2 resonance of d(GpA) at 7.81 (3′-AH2) and a resonance at $\delta = 10.32$ ppm (N1H 3′-A) ($^3J_{^1H-^1H} \approx 3$ Hz).[47,76] Likewise, in the [^{1}H–^{1}H] DQF-COSY spectrum of [Rh_2(DTolF)$_2$-{d(ApG)}] in CD_3CN at −38 °C, cross-peaks are observed between the 5′-A H2 resonance of d(ApG) at $\delta = 7.62$ ppm and the 5′-A N1H resonance at $\delta = 7.29$ ppm (Figure 5).[76] The upfield value for the 5′-A N1H imino proton resonance of [Rh_2(DTolF)$_2${d(ApG)}], as compared to the 3′-A N1H imino proton of [Rh_2(DTolF)$_2${d(GpA)}], is attributed to the shielding effect on the 5′-A ring by the tolyl group of the formamidinate bridge, as indicated by the models.

The previous H2/N1H DQF-COSY cross-peaks provide unambiguous evidence that the N1 sites of the adenine bases in [Rh_2(DTolF)$_2${d(GpA)}] and [Rh_2(DTolF)$_2${d-(ApG)}] are protonated and thus present in the rare imino form, which is stabilized by the bidentate metalation of the N7 and N6 sites.[25,47,49] Moreover, in the ROESY spectra in CD_3CN at −38 °C, ROESY cross-peaks are observed between the 3′-A N1H ($\delta = 10.32$ ppm) with 3′-A N6H ($\delta = 6.98$ ppm) resonances (for [Rh_2(DTolF)$_2${d(GpA)}]) and between 5′-A N1H ($\delta = 7.29$ ppm) with 5′-A N6H ($\delta = 7.10$ ppm) resonances (for [Rh_2(DTolF)$_2${d(ApG)}]), further confirming protonation of the adenine N1H sites of the adducts (the X-ray crystallographic study of *cis*-[Rh_2-

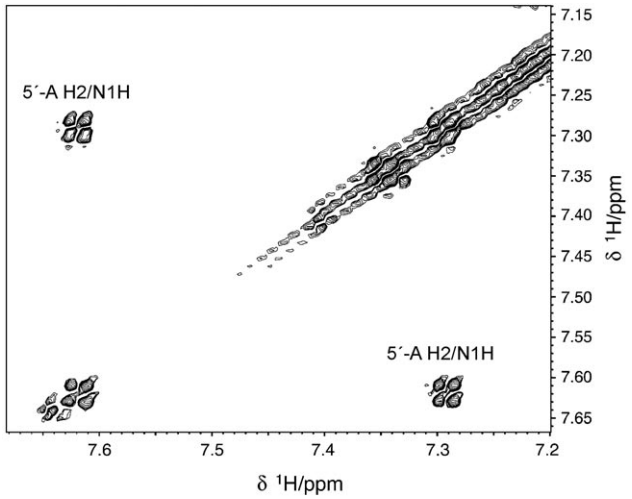

Figure 5. [^{1}H–^{1}H] DQF-COSY spectrum of [Rh_2(DTolF)$_2${d(ApG)}] in CD_3CN at −38 °C.

(DTolF)$_2$(9-EtAdeH)$_2$](BF$_4$)$_2$ showed that the adenine N1H–N6H distance is 2.25 Å[40,41]).

^{31}P NMR spectroscopy: The 1D ^{31}P NMR spectra of [Rh_2(DTolF)$_2${d(GpA)}] and [Rh_2(DTolF)$_2${d(ApG)}] in CD_3CN display resonances at $\delta = -3.16$ (Figure 4) and −2.29 ppm, (Table 1), respectively, downfield from the respective free dinucleotides d(GpA) and d(ApG) at $\delta = -4.06$ and −4.09 ppm, respectively; this behavior is typical of HH adduct phosphate groups, which resonate approximately 1 ppm downfield from the free dinucleotides.[22–24] Downfield shifts of the ^{31}P NMR signals in DNA are typically characterized by changes in the R–O–P–OR′ torsion angles.[77]

Molecular modeling: Each HH1R, HH2R, HH1L, and HH2L conformer[24] of the tethered adducts [Rh_2(DTolF)$_2$-{d(GpA)}] and [Rh_2(DTolF)$_2${d(ApG)}] was independently constructed and subjected to simulated annealing calculations. Initial right- and left-handed models produced minimized conformers with the same canting as the original models only. The lowest energy HH1R variant for [Rh_2(DTolF)$_2${d(GpA)}] (Figure 6, upper panel) is more stable by 3.5 kcal mol^{-1} than the lowest energy HH2L. In the case of [Rh_2(DTolF)$_2${d(ApG)}], the lowest energy HH1R variant (Figure 6, lower panel) is higher in energy by 4.1 kcal mol^{-1} than the lowest energy HH2L conformer, but the HH2L conformer was not considered because the NMR spectroscopic data did not support a left-handed conformer. The conformational features of the [Rh_2(DTolF)$_2${d(GpA)}] and [Rh_2(DTolF)$_2${d(ApG)}] adducts, suggested by the NMR spectroscopic data, were reproduced well by the calculations.

The H8/H8 cross-peaks in the 2D ROESY NMR spectra of [Rh_2(DTolF)$_2${d(GpA)}] and [Rh_2(DTolF)$_2${d(ApG)}] (Figure 3) are in accordance with the H8/H8 distances for the lowest energy HH1R models (~3.21 and ~3.25 Å,

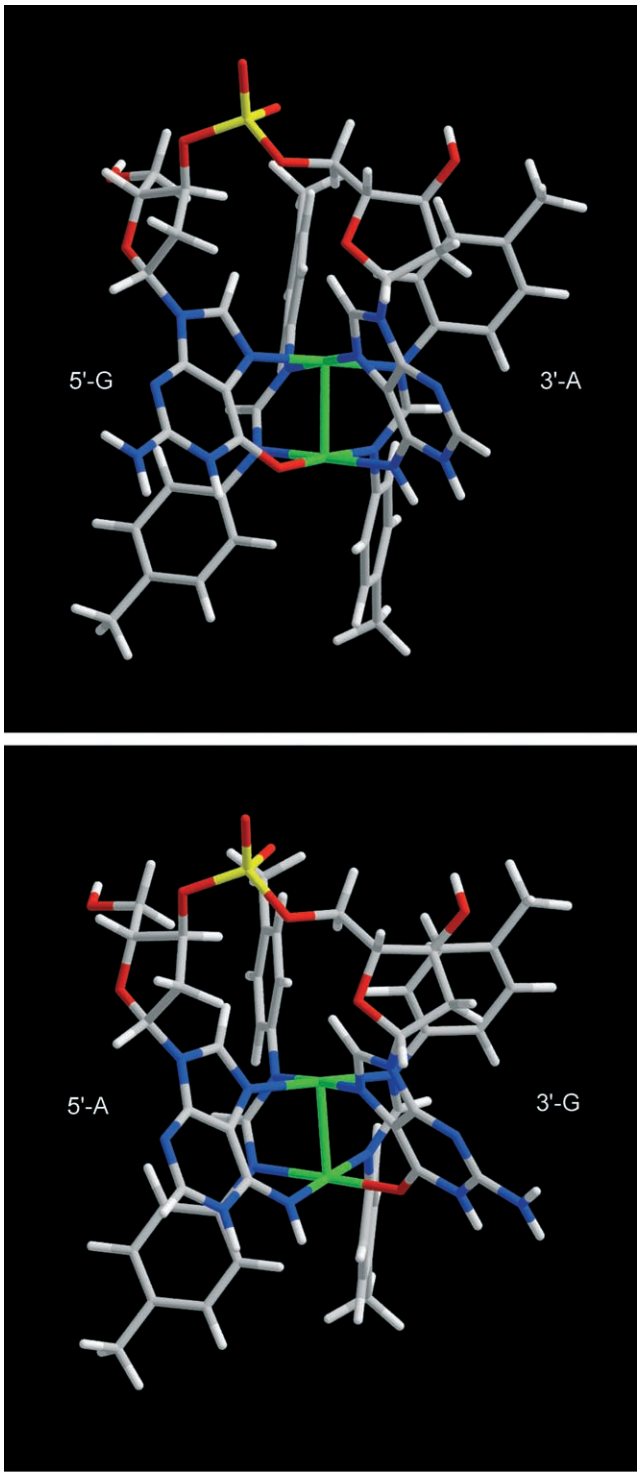

Figure 6. Lowest energy conformers, resulting from simulated annealing calculations, for the HH1R variants of $[Rh_2(DTolF)_2\{d(GpA)\}]$ (upper panel) and $[Rh_2(DTolF)_2\{d(ApG)\}]$ (lower panel). For each adduct, the 5′ residue is positioned to the left and the 3′ residue is the more canted base. Rh green, N blue, O red, P yellow, C gray, H white.

respectively; Table 2) (see above). The NMR spectroscopic data of the two adducts support the presence of all deoxyribose residues in the *anti* orientation with respect to the glycosyl bonds. For both dinucleotide adducts, the interproton H8/H3′ distances (2.35 Å) for the lowest energy HH1R conformers corroborate strong H8/H3′ ROESY cross-peaks and thus N-type sugar pucker geometries for the 5′ sugar residues. Moreover, as indicated in the model for $[Rh_2(DTolF)_2\{d(ApG)\}]$, the 5′-A N1H imino proton is in the shielding cone of the formamidinate tolyl group (Figure 6, bottom panel), thus giving rise to an upfield-shifted resonance at $\delta = 7.29$ ppm in the ^{1}H NMR spectrum (Table 1). Similarly to the dinucleotide adducts $[Rh_2(O_2CCH_3)_2\{d(GpG)\}]$,[22] $[Rh_2(O_2CCH_3)_2\{d(pGpG)\}]$,[23] $[Rh_2(DTolF)_2\{d(GpG)\}]$,[24] $[Rh_2(DTolF)_2\{d(ApA)\}]$,[25] and *cis*-$[Pt(NH_3)_2\{d(pGpG)\}]$,[23] the purine bases in the minimized $[Rh_2(DTolF)_2\{d(GpA)\}]$ and $[Rh_2(DTolF)_2\{d(ApG)\}]$ HH1R conformers are destacked with interbase dihedral angles between 3′-B and 5′-B $\approx$ 72–74°.

Discussion

Conformational features of $[Rh_2(DTolF)_2\{d(GpA)\}]$ and $[Rh_2(DTolF)_2\{d(ApG)\}]$: The dinucleotide aromatic protons in the tethered adducts $[Rh_2(DTolF)_2\{d(GpA)\}]$ and $[Rh_2(DTolF)_2\{d(ApG)\}]$ are nonequivalent. Both adducts give rise to well-dispersed H8 proton resonances and relatively intense H8/H8 NOE cross-peaks (Figure 3), which are consistent with HH base conformation.[31] Based on the 2D NMR spectroscopic data analysis for each adduct, $[Rh_2(DTolF)_2\{d(GpA)\}]$ and $[Rh_2(DTolF)_2\{d(ApG)\}]$, the downfield and upfield H8 resonances are assigned to the 5′ and 3′ base H8 protons, respectively (Table 1). In addition to the deshielding effect of the metal on both rings, each base experiences an upfield shifting effect as a result of the ring-current anisotropy of the other *cis* base.[38,39,78] In compliance with the recently assessed rules for base canting in platinum compounds,[32,36] the H8 resonance of the more canted base moves upfield as a result of the ring current effects of the less canted base.[79] As the 3′ base H8 resonance is more upfield than the 5′ base H8 resonance for both dinucleotide adducts (Table 1), it is concluded that the 3′ base is more canted than the 5′ base in each adduct (Scheme 5). Taking into consideration both the experimental evidence from the NMR spectroscopic data and the molecular modeling results, the conformers present in solution for the $[Rh_2(DTolF)_2\{d(GpA)\}]$ and $[Rh_2(DTolF)_2\{d(ApG)\}]$ adducts are assigned to the right-handed variant HH1R for each adduct (Scheme 5, Table 2). HH1R variants have precedent for dirhodium acetate d(GpG),[22] formamidinate d(GpG)[24] and d(ApA)[25] dinucleotide adducts. As in the cases of the d(GpG) and d(ApA) dirhodium adducts, the bulk and the nonlabile character of the formamidinate groups slow down the possible dynamic processes for the mixed base dinucleotide adducts and favor the formation of the HH1R conformers.[24,25] It is therefore evident that the dirhodium formamidinate adducts give rise to R minihelix variants and, in this respect, are good models for the duplex DNA cisplatin cross-link lesion, because in duplexes with

Table 2. Summary of lowest energy dirhodium formamidinate dinucleotide adducts.

Model	Percent [%][a]	Energy [kcal mol^{-1}]	χ [°][b]		P [°][c]		5′-B H8/ 3′-B H8 [Å]	3′-B/5′-B Dihedral angle[°][d]
			5′-B	3′-B	5′-B	3′-B		
[Rh_2(DTolF)$_2${d(GpA)}] HH1R[a]	100	306.9	−135	−161	20	162	3.21	73.4
[Rh_2(DTolF)$_2${d(ApG)}] HH1R[a]	100	306.8	−137	−163	19	169	3.25	71.7
[Rh_2(DTolF)$_2${d(GpG)}] HH1R[a,e]	100	300.7	−137	−146	20	12	3.30	75.9
[Rh_2(DTolF)$_2${d(ApA)}] HH1R[a,f]	100	297.5	−135	−163	36	163	3.20	73.8

[a] Experimentally detected. [b] χ = O4′–C1′–N9–C4; $|\chi| > 90°$ and $|\chi| < 90°$ correspond to the *anti* and *syn* range respectively, for torsion angles $-180° < \chi < +180°$. [c] P = pseudorotation phase angle calculated from the equation $\tan P = (\nu_4 + \nu_1) - (\nu_3 + \nu_0)/[2\nu_2(\sin 36° + \sin 72°)]$ (ν_{0-4} are endocyclic sugar torsion angles; $0° \le P \le 36°$ ($\pm 18°$) corresponds to an N sugar, whereas $144° \le P \le 190°$ ($\pm 18°$) indicates an S sugar; if $\nu_2 < 0$, $P = P + 180°$. [d] Dihedral angles between 5′-B and 3′-B bases were calculated by using atoms N1, N3, N7 of each purine ring. [e] Reported in reference [24]. [f] Reported in reference [25].

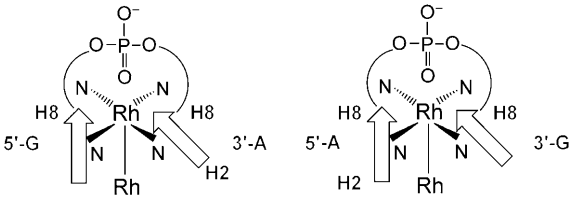

Scheme 5. Head-to-head (HH) variants of [Rh_2(DTolF)$_2${d(GpA)}] and [Rh_2(DTolF)$_2${d(ApG)}] with right (R) canting. Canting arises from the fact that the purine bases are not oriented exactly perpendicular to the N7-Rh-N7 plane. The 1 in HH1R refers to models with the 5′-base positioned to the left. The two rhodium atoms are depicted as face-to-face square planes with the Rh atom attached to the purine N7 atoms shown in the front and the N atoms of the attached bridging formamidinate groups in the back; to show the structures clearly, the remaining coordination sites for the second Rh atom are not shown. Each A base is indicated by an arrow having H8 at the tip and H2 at the other end, whereas each G base is indicated with H8 at the tip. A complete description of all the possible variants is given in reference [24].

the *cis*-[$Pt(NH_3)_2${d(GpG)}] moiety, the HH1R variants appear to dominate.[33,34,80]

The cisplatin[34] and Ru(II)-dimethyl sulfoxide[81] d(ApG) dinucleotide adducts are also right-handed conformers and their metalated fragments have been isolated with both d(ApG) and d(GpA) dinucleotides , a fact that can be attributed to the conformational freedom of the smaller DNA fragments.[54] It is well-established, however, that cisplatin forms 1,2-intrastrand adducts with d(ApG) but not with d(GpA) in full-length double-stranded DNA.[51,52,68,82] The preference of the d(ApG) over the d(GpA) adduct, in the case of cisplatin interacting with double-stranded DNA, is attributed to the strong hydrogen bond established between the axial ammine ligand and the phosphate backbone in the d(ApG) adduct, which reduces the energy of the relevant transition state by 9–10 kcal mol^{-1}.[52] In the present study of the dirhodium formamidinate unit with the d(GpA) and d(ApG) dinucleotides, both reactions take place, but the rate is slower for d(ApG) than for d(GpA), which is also the case with the relevant Ru^{II}–dimethyl sulfoxide complexes.[81] Although it is known that, in the absence of guanine bases, 5′-A is a primary target for dirhodium tetraacetate[15] and the energy of the transition state for the reaction to form the bridging adenine N6/N7 adduct with the dirhodium unit is significantly lowered in the presence of strong *trans*-labilizing ligands, such as formamidinate groups,[49] further theoretical studies are necessary to elucidate the mechanism of interaction between the dirhodium unit and short or longer DNA fragments.

In regards to the deoxyribose conformations for the adducts, the 2D NMR spectroscopic data for [Rh_2(DTolF)$_2${d(GpA)}] and [Rh_2(DTolF)$_2${d(ApG)}] support *anti* orientation of both the 5′- and 3′- sugar residues about the glycosyl bonds, retention of the 3′-deoxyribose residues in the native S-type (C2′-endo) conformations, and adoption of N-type (C3′-endo) conformations for the 5′-sugar residues. The aforementioned features of [Rh_2(DTolF)$_2${d(GpA)}] and [Rh_2(DTolF)$_2${d(GpA)}] bear close resemblance to those of cisplatin with d(GpG), which typically are HH cross-linked adducts with *anti/anti* 5′-G and 3′-G sugar residues in the N and S conformations, respectively.[83] The change in sugar puckering geometry of the 5′-deoxyribose residues in the d(GpA), d(ApG), d(GpG)[22–24] and d(ApA)[25] dirhodium adducts is observed in all bifunctional adducts of platinum. Theoretical studies support the important role of this change to allow for a greater tilt angle of the two purine bases and a more relaxed coordination geometry at the metal centers.[52]

Bidentate binding and tautomers of the guanine and adenine bases: As previously reported for [Rh_2(DTolF)$_2$(9-EtGuaH)$_2$](BF_4)$_2$ (9-EtGuaH: 9-ethylguanine) and [Rh_2(DTolF)$_2${d(GpG)}],[24] the pH-dependent ^{1}H NMR titration curves for the H8 guanine resonances of [Rh_2(DTolF)$_2${d(GpA)}] and [Rh_2(DTolF)$_2${d(ApG)}] (Figures 1 and 2) indicate the absence of N7 protonation at low pH values as well as a substantial enhancement in the acidity of the guanine N1H sites ($pK_a \approx 7.4$) in the dirhodium mixed purine adducts as compared to the free dinucleotides.[22,23] The latter effects are induced by the purine bidentate binding to the rhodium centers by N7 and O6 (also confirmed by the X-ray crystallographic study of HH *cis*-[Rh_2(DTolF)$_2$(9-EtGuaH)$_2$($NCCH_3$)](BF_4)$_2$)[40] and indicate the presence of the guanine bases in the enolate form at physiological pH values.[22]

The pH-dependence curves of the 3′-A and 5′-A H2 and H8 ^{1}H NMR signals in 4:1 CD_3CN/D_2O for the adducts [Rh_2(DTolF)$_2${d(GpA)}] and [Rh_2(DTolF)$_2${d(ApG)}],

(Figures 1 and 2), indicate that the N1H groups are deprotonated at pK_a 7.0–7.1, that is, at considerably reduced pH values as compared to N1 (de)protonation of the adenosine imino tautomer (estimated to be considerably higher than 11 in CD_3CN/D_2O).[61,62,70] The decrease in the basicity of the adenine N1H sites in the adducts has been correlated to the presence of the rare imino form of the base, and results from N6/N7 bidentate binding to the metal (Scheme 4).[45] A similar behavior of the N1 sites, resulting from the metal binding of the adenine N6 and N7 has also been recorded in $[Rh_2(DTolF)_2\{d(ApA)\}]$ and HT *cis*-$[Rh_2(DTolF)_2(9\text{-}EtAdeH)_2](BF_4)_2$,[25] for which the X-ray structure has been determined.[40,41] As indicated in the previous X-ray structure as well as in the models for $[Rh_2(DTolF)_2\{d(GpA)\}]$ and $[Rh_2(DTolF)_2\{d(ApG)\}]$ (Figure 6), only the *anti* orientation is possible for the metal at N6 and the protonated N1 as a result of the bidentate N6/N7 binding.[25] The presence of the adenine base in the rare imino form, resulting from bidentate metalation of the N6/N7 sites in $[Rh_2(DTolF)_2\{d(GpA)\}]$ and $[Rh_2(DTolF)_2\{d(ApG)\}]$ is further corroborated by the H2/N1H cross-peaks in the [^{1}H–^{1}H] DQF-COSY spectra (Figure 5 for $[Rh_2(DTolF)_2\{d(ApG)\}]$) and the N1H/N6H cross-peaks in the ROESY spectra of the adducts in CD_3CN at −38 °C.[25,47] The ROESY data provide unambiguous evidence that the N1 sites of the adenine bases in $[Rh_2(DTolF)_2\{d(GpA)\}]$ and $[Rh_2(DTolF)_2\{d(ApG)\}]$ are protonated below the determined pK_a values (~7.0–7.1). The imino form of adenine in metalated DNA lesions may result in nucleobase mispairing by inducing AT⟶CG transversions or AT⟶GC transitions, which can be lethal if not repaired.[45,46,70,84–86]

Conclusion

The present study of the dinucleotide adducts $[Rh_2(DTolF)_2\{d(GpA)\}]$ and $[Rh_2(DTolF)_2\{d(ApG)\}]$ provides unambiguous evidence that the mixed DNA–purine fragments span the Rh−Rh bond in *eq* positions with N7/O6 and N7/N6 bridges for the guanine and adenine bases, respectively. Coordination of the adenine N7 and N6 sites to the rhodium atoms in the adducts induces formation of the metal-stabilized rare imino tautomer of adenine with a concomitant substantial decrease in the basicity of the N1H sites.[25] Similarly, the N7/O6 binding of the guanine bases induces a notable increase in the acidity of the N1H site (and formation of the enolate form).[24] The shifting of the pK_a values of the bases in the physiological range and the stabilization of rare base tautomers, resulting from binding of the nucleotides to the dirhodium core, have a major influence on the hydrogen-bonding properties of the bases with important biological implications.[45,46,70]

In the dinucleotide adducts $[Rh_2(DTolF)_2\{d(GpA)\}]$ and $[Rh_2(DTolF)_2\{d(ApG)\}]$, the two rhodium centers are favorably positioned to accommodate the bidentate binding of the purine bases, which are almost completely destacked (dihedral angle 3′-B/5′-B = 72–74°) as compared to B DNA. The backbone tether dictates the HH nature of the adducts, whereas the bulky and nonlabile nature of the formamidinate bridging groups leads to right-handed HH1R conformers (Scheme 5, Table 2) in solution, as in the cases of the homopurine $[Rh_2(DTolF)_2\{d(GpG)\}]$[24] and $[Rh_2(DTolF)_2\{d(ApA)\}]$[25] adducts. The dirhodium formamidinate core with purine dinucleotides gives rise to R minihelix variants and thus provides good models for the duplex DNA–cisplatin d(GpG) cross-link lesions responsible for the antitumor properties of the drug. The other conformational features of the dirhodium adducts also resemble those of known platinum d(GpG) adducts: all sugar residues have *anti* orientation about the glycosyl bonds and the 5′ bases of the adducts adopt N-type conformations to accommodate the base binding to the metal centers. It remains to be determined if the antitumor active compound *cis*-$[Rh_2(DTolF)_2(O_2CCF_3)_2(H_2O)_2]$ and its derivatives form relevant cross-links with d(GpA) and d(ApG) sites in double-stranded DNA.

Experimental Section

The starting material $RhCl_3{\cdot}xH_2O$ was obtained from Pressure Chemical Co. (Pittsburgh, PA) and was used without further purification. The complex *cis*-$[Rh_2(DTolF)_2(NCCH_3)_6](BF_4)_2$ was prepared according to literature procedures.[40] The dinucleotide d(GpA) was purchased as the crude 5′-O-dimethoxytrityl (DMT) protected material from the Gene Technologies Laboratory at Texas A&M University. It was purified by reverse-phase HPLC and used as the sodium salt. The dinucleotide d(ApG) was purchased from Sigma as the ammonium salt and was used as received. Concentrations of the free dinucleotides were determined by UV spectroscopy at 260 nm ($\varepsilon_{260} = 2.7\times10^4\,M^{-1}\,cm^{-1}$). Deuterium oxide ($D_2O$, 99.996%), deuterated acetonitrile (CD_3CN, 99.8%), deuterium chloride (DCl, 99.5%), sodium deuteroxide (NaOD, 99.5%) and DSS (sodium 2,2-dimethyl-2-silapentane-5-sulfonate) were purchased from Cambridge Isotope Laboratories. TMP {$(CH_3O)_3PO$} was purchased from Aldrich.

Syntheses

a) $[Rh_2(DTolF)_2\{d(GpA)\}]$: In a typical reaction, $[Rh_2(DTolF)_2(NCCH_3)_6](BF_4)_2$ (2.4 μmol) in CD_3CN (200 μL, brown solution) was treated with of d(GpA) (2.4 μmol) in D_2O (50 μL). Upon mixing the two solutions, a white precipitate formed. After incubating the sample at 37 °C for two days, the white solid dissolved completely and the color of the solution changed from brown to olive green. The progress of the reaction was monitored by ^{1}H NMR spectroscopy until no free d(GpA) could be detected. The reaction was complete in approximately 10 days. MS-ESI (positive ion mode) *m/z*: 1232 ($[Rh_2(DTolF)_2\{d(GpA)\}]^+$, see Supporting Information, Figure S1).

b) $[Rh_2(DTolF)_2\{d(ApG)\}]$: In a typical reaction, $[Rh_2(DTolF)_2(NCCH_3)_6](BF_4)_2$ (2.4 μmol) in CD_3CN (200 μL, brown solution) was treated with d(ApG) (2.4 μmol) in D_2O (50 μL). Upon mixing the two solutions, a white precipitate formed. After incubating the sample at 37 °C for two days, the white solid dissolved completely and the color of the solution changed from brown to dark green/brown. The progress of the reaction was monitored by ^{1}H NMR spectroscopy until no free d(ApG) could be detected. The reaction is complete in approximately 12 days. MS-ESI (negative ion mode) *m/z*: 1231 ($[Rh_2(DTolF)_2\{d(ApG)\}\text{-}H]^-$, see Supporting Information, Figure S2).

Instrumentation: 1D ^{1}H NMR spectra were recorded on a 500 MHz Varian Inova spectrometer with a 5 mm switchable probehead. The ^{1}H NMR spectra were typically recorded with 5000 Hz sweep width and 32 K data points. A presaturation pulse to suppress the water peak was used when necessary. The 1D ^{31}P NMR spectra were recorded on a

Varian 300 MHz spectrometer operating at 121.43 MHz for ^{31}P. The ^{1}H NMR spectra were referenced to the residual proton impurity of CD_3CN. Trimethyl phosphate (TMP, $\delta = 0$ ppm) was used as an external reference for the ^{31}P NMR spectra. The 1D NMR data were processed using the Varian VNMR 6.1b software.

2D NMR data were collected at 10 °C on a Varian Inova 500 MHz spectrometer equipped with a triple-axis gradient penta probe. In general, the homonuclear experiments were performed with a spectral width of approximately 5000 Hz in both dimensions, while some high resolution 2D [^{1}H–^{1}H] DQF-COSY spectra were collected with 3000 Hz spectral width. 2D [^{1}H–^{1}H] ROESY spectra were collected with mixing times of 150 and 300 ms. A minimum of 2048 points were collected in t_2 with at least 256 points in t_1 and 32–64 scans per increment. 2D [^{1}H–^{1}H] DQF-COSY spectra, collected with ^{31}P decoupling in both dimensions, resulted in a 1228 × 440 data matrix with 40 scans per increment. 2D [^{1}H–^{31}P] HETCOR experiments were collected with 2048 points in t_2, 112 points in t_1 with 512 scans per increment. The ^{31}P NMR spectral width was approximately 1500–3500 Hz. All data sets were processed using a 90° phase-shifted sine-bell apodization function and were zero filled. The baselines were corrected with first or second order polynomials. Two-dimensional (2D) NMR data were processed using the program nmrPipe.[87]

The pH values of the samples were recorded on a Corning pH meter 430 equipped with a MI412 microelectrode probe by Microelectrodes, Inc. The pH values of the samples were monitored in acetonitrile/water solutions; calibration of the MI412 glass microelectrode probe was performed in standard aqueous buffer solutions. The difference in the pH value of the buffer measured in an aqueous solution and its pH* value in an acetonitrile/water mixture primarily depends on the liquid-junction potential of the electrode, which is negligible for the electrode used. It has been reported that, for electrodes with a negligible liquid-junction potential, the pH and pH* values for various buffers measured in aqueous and acetonitrile/water mixtures, respectively, differ by 0.01 to 0.2 pH units, which is the precision expected for measurements in non-aqueous and mixed solvents.[63,88] The pH-dependence of the chemical shifts for the purine proton nuclei H8 and H2 was monitored by adding trace amounts of DCl and NaOD solutions to the samples. No correction was applied to the pH values for deuterium isotope effects on the glass electrode. The pH titration curves were fitted to the Henderson–Hasselbalch equation using the program Kaleidagraph, with the assumption that the detected chemical shifts are weighted averages according to the populations of the protonated and deprotonated species. The $pK_{a(s)}$ values for the dirhodium adducts determined in acetonitrile/water mixtures, however, are not comparable with the reported $pK_{a(w)}$ values of similar systems measured in water. They are only comparable to the $pK_{a(s)}$ values of similar systems in acetonitrile/water mixtures[24,25] or to the free ligands estimated in the same acetonitrile/water solvent system, as the range of the pH scale for acetonitrile (the pK_a value for acetonitrile is 28.5) is different from that of water.[89]

Electrospray mass spectra were acquired on an MDS Sciex API QStar Pulsar mass spectrometer (Toronto, Ontario, Canada) using an electrospray ionization source. The UV spectra were collected with a Shimadzu UV 1601PC spectrophotometer.

Molecular modeling: Molecular modeling results were obtained using the software package Cerius^2 4.6 (Accelrys Inc., San Diego). To sample the conformational space of each compound, simulated annealing (SA) calculations in the gas phase were performed using the Open Force Field (OFF) program, with a modified version of the Universal Force Field (UFF).[90–92] The SA was carried out for 80.0 ps, over a temperature range of 300–500 K, with $\Delta T = 50$ K, using the Nosé temperature thermostat, a relaxation time of 0.05 ps and a time step of 0.001 ps. The compounds were minimized (quenched) after each annealing cycle, producing 200 minimized structures. UFF is parameterized for octahedral Rh^{III}, whereas the molecules in the present study are metal–metal bonded Rh^{II} compounds in a paddlewheel structure with axial ligands. To account for the difference in the oxidation state and the coordination environment of the metal, the valence bond parameter was modified. The appropriate valence bond parameters for these types of complexes were previously developed[22,23] and were appropriately modified for the $Rh{-}N_{DTolF}$ bond by taking into consideration the crystal structures of HH *cis*-$[Rh_2(DTolF)_2(9\text{-}EtGuaH)_2(NCCH_3)]^{2+}$ and HT *cis*-$[Rh_2(DTolF)_2(9\text{-}EtAdeH)_2]^{2+}$.[40,41] The original valence bond value of 1.3320 Å for Rh^{III} was set to 1.2550 Å and all other parameters were unmodified. The bond orders for all bonds, except those including the Rh atoms, were calculated using the OFF bond order settings. The Rh–Rh and metal–ligand bond orders were set to 1.0 and 0.5, respectively. The calculated Rh–Rh bond length obtained for the lowest energy conformer of HT *cis*-$[Rh_2(DTolF)_2(9\text{-}EtAdeH)_2]^{2+}$ is 2.50 Å.[40,41] The Rh–Rh, Rh–N6/N7(adenine) and $Rh{-}N_{DTolF}$ bond lengths are within 0.01, 0.08, and 0.1 Å, respectively, of the crystal structure values for HT *cis*-$[Rh_2(DTolF)_2(9\text{-}EtAdeH)_2]^{2+}$.[40,41] The distances from the crystal structure of HH *cis*-$[Rh_2(DTolF)_2(9\text{-}EtGuaH)_2(NCCH_3)]^{2+}$ were not used, owing to the poor quality of the data.[40]

Acknowledgements

Dr. K. M. Koshlap is acknowledged for assistance with collection of the 2D NMR data. Dr. Lisa Pérez is acknowledged for assistance with the molecular modeling; the Laboratory for Molecular Simulations at Texas A&M University is acknowledged for providing software and computer time. Use of the TAMU/LBMS-Applications Laboratory (Laboratory of Biological Mass Spectroscopy) is also acknowledged. The NMR instrumentation in the Chemistry Department at Texas A&M University was funded by the National Science Foundation (CHE-0077917). The NMR instrumentation in the Biomolecular NMR Laboratory at Texas A&M University was supported by a grant from the National Science Foundation (DBI-9970232) and the Texas A&M University System. KRD thanks the Welch Foundation (A-1449) for financial support.

[1] H. T. Chifotides, K. R. Dunbar, "Rhodium Compounds" in "*Multiple Bonds Between Metal Atoms*", *Chapter 12* (Eds.: F. A. Cotton, C. Murillo, R. A. Walton), Springer-Science and Business Media, Inc., New York, **2005**, pp. 465–589.
[2] R. G. Hughes, J. L. Bear, A. P. Kimball, *Proc. Am. Assoc. Cancer Res.* **1972**, *13*, 120.
[3] R. A. Howard, A. P. Kimball, J. L. Bear, *Cancer Res.* **1979**, *39*, 2568–2573.
[4] A. Erck, L. Rainen, J. Whileyman, I.-M. Chang, A. P. Kimball, J. L. Bear, *Proc. Soc. Exp. Biol. Med.* **1974**, *145*, 1278–1283.
[5] J. L. Bear, H. B. Gray, Jr., L. Rainen, I. M. Chang, R. Howard, G. Serio, A. P. Kimball, *Cancer Chemother. Rep.* **1975**, *59*, 611–620.
[6] R. A. Howard, E. Sherwood, A. Erck, A. P. Kimball, J. L. Bear, *J. Med. Chem.* **1977**, *20*, 943–946.
[7] S. Zyngier, E. Kimura, R. Najjar, *Braz. J. Med. Biol. Res.* **1989**, *22*, 337–344.
[8] J. L. Bear, *Precious Metals 1985: Proceedings of the Ninth International Precious Metals Conference* (Eds.: E. D. Zysk, J. A. Bonucci), Int. Precious Metals, Allentown, PA, **1986**, p. 337.
[9] A. R. de Souza, E. P. Coelho, S. B. Zyngier, *Eur. J. Med. Chem.* **2006**, *41*, 1214–1216.
[10] J. M. Asara, J. S. Hess, E. Lozada, K. R. Dunbar, J. Allison, *J. Am. Chem. Soc.* **2000**, *122*, 8–13.
[11] H. T. Chifotides, J. M. Koomen, M. Kang, K. R. Dunbar, S. Tichy, D. H. Russell, *Inorg. Chem.* **2004**, *43*, 6177–6187.
[12] S. U. Dunham, H. T. Chifotides, S. Mikulski, A. E. Burr, K. R. Dunbar, *Biochemistry* **2005**, *44*, 996–1003.
[13] H. T. Chifotides, K. R. Dunbar, *Acc. Chem. Res.*, **2005**, *38*, 146–156, and references therein.
[14] H. T. Chifotides, K. R. Dunbar, *Angew. Chem.* **2006**, *118*, 6294–6297; *Angew. Chem. Int. Ed.* **2006**, *45*, 6148–6151.
[15] M. Kang, H. T. Chifotides, K. R. Dunbar, *Biochemistry*, **2008**, *47*, 2265–2276.
[16] P. N. Rao, M. L. Smith, S. Pathak, R. A. Howard, J. L. Bear, *J. Natl. Cancer Inst.* **1980**, *64*, 905–911.

[17] L. D. Dale, T. M. Dyson, D. A. Tocher, J. H. Tocher, D. I. Edwards, *Anti-Cancer Drug Des.* **1989**, *4*, 295–302.
[18] H. T. Chifotides, P. K.-L. Fu, K. R. Dunbar, C. Turro, *Inorg. Chem.* **2004**, *43*, 1175–1183.
[19] V. Fimiani, T. Ainis, A. Cavallaro, P. Piraino, *J. Chemother.* **1990**, *2*, 319–326.
[20] D. V. Deubel, H. T. Chifotides, *Chem. Commun.* **2007**, 3438–3440.
[21] A. M. Angeles-Boza, H. T. Chifotides, J. D. Aguirre, A. Chouai, P. K.-L. Fu, K. R. Dunbar, C. Turro, *J. Med. Chem.* **2006**, *49*, 6841–6847.
[22] H. T. Chifotides, K. M. Koshlap, L. M. Pérez, K. R. Dunbar, *J. Am. Chem. Soc.* **2003**, *125*, 10703–10713.
[23] H. T. Chifotides, K. M. Koshlap, L. M. Pérez, K. R. Dunbar, *J. Am. Chem. Soc.* **2003**, *125*, 10714–10724.
[24] H. T. Chifotides, Kim R. Dunbar, *Chem. Eur. J.* **2006**, *12*, 6458–6468.
[25] H. T. Chifotides, K. R. Dunbar, *J. Am. Chem. Soc.* **2007**, *129*, 12480–12490.
[26] D. Wang, S. J. Lippard, *Nat. Rev. Drug Discovery* **2005**, *4*, 307–320.
[27] J. Reedijk, *Proc. Natl. Acad. Sci. USA* **2003**, *100*, 3611–3616.
[28] K. R. Barnes, S. J. Lippard, *Met. Ions Biol. Syst.* **2004**, *42*, 143–177.
[29] L. Kelland *Nature Rev. Cancer*, **2007**, *7*(8), 573–584.
[30] H. Sugiyama, I. Saito, *J. Am. Chem. Soc.* **1996**, *118*, 7063–7068.
[31] a) For dirhodium adducts with bridging ligands possessing different types of donor atoms, for example, 9-ethylguanine or 9-ethyladenine, the compound is designated as HH or HT, according to whether the identical atoms of the two ligands are bound to the same or to opposite metal atoms, respectively. b) R (as in HH1R) refers to the relative base canting. Canting arises from the fact that the purine bases are not oriented exactly perpendicular to the N7-Rh-N7 plane (see Scheme 5).[24]
[32] S. O. Ano, F. P. Intini, G. Natile, L. G. Marzilli, *J. Am. Chem. Soc.* **1998**, *120*, 12017–12022.
[33] J. Kozelka, M.-H. Fouchet, J.-C. Chottard, *Eur. J. Biochem.* **1992**, *205*, 895–906.
[34] D. Lemaire, M.-H. Fouchet, J. Kozelka, *J. Inorg. Biochem.* **1994**, *53*, 261–271.
[35] L. G. Marzilli, S. O. Ano, F. P. Intini, G. Natile, *J. Am. Chem. Soc.* **1999**, *121*, 9133–9142, and references therein.
[36] K. M. Williams, L. Cerasino, G. Natile, L. G. Marzilli, *J. Am. Chem. Soc.* **2000**, *122*, 8021–8030.
[37] S. T. Sullivan, A. Ciccarese, F. P. Fanizzi, L. G. Marzilli, *J. Am. Chem. Soc.* **2001**, *123*, 9345–9355, and references therein.
[38] G. Natile, L. G. Marzilli, *Coord. Chem. Rev.* **2006**, *250*, 1315–1331, and references therein.
[39] R. Ranaldo, N. Margiotta F. P. Intini, C. Pacifico, G. Natile, *Inorg. Chem.* **2008**, *47*, 2820–2830.
[40] K. V. Catalan, J. S. Hess, M. M. Maloney, D. J. Mindiola, D. L. Ward, K. R. Dunbar, *Inorg. Chem.* **1999**, *38*, 3904–3913.
[41] K. V. Catalan, D. J. Mindiola, D. L. Ward, K. R. Dunbar, *Inorg. Chem.* **1997**, *36*, 2458–2460.
[42] M. Hanus, M. Kabelác, J. Rejnek, F. Ryjácek, P. Hobza, *J. Phys. Chem. B* **2004**, *108*, 2087–2097.
[43] A. Laxer, D. T. Major, H. E. Gottlieb, B. Fischer, *J. Org. Chem.* **2001**, *66*, 5463–5481.
[44] B. Lippert, *Coord. Chem. Rev.* **2000**, *200–202*, 487–516.
[45] B. Lippert, *Prog. Inorg. Chem.* **2005**, *54*, 385–447.
[46] J. Sponer, J. E. Sponer, L. Gorb, J. Leszczynski, B. Lippert, *J. Phys. Chem. A* **1999**, *103*, 11406–11413.
[47] A. C. G. Hotze, M. E. T. Broekhuisen, A. H. Velders, K. van der Schilden, J. G. Haasnoot, J. Reedijk, *Eur. J. Inorg. Chem.* **2002**, 369–376.
[48] A. C. G. Hotze, M. E. T. Broekhuisen, A. H. Velders, H. Kooijman, A. L. Spek, J. G. Haasnoot, J. Reedijk, *J. Chem. Soc. Dalton Trans.* **2002**, 2809–2810.
[49] D. V. Deubel, *J. Am. Chem. Soc.* **2008**, *130*, 665–675.
[50] A. M. J. Fichtinger-Schepman, J. L. van der Veer, J. H. J. den Hartog, P. H. M. Lohman, J. Reedijk, *Biochemistry* **1985**, *24*, 707–713.
[51] M.-H. Baik, R. A. Friesner, S. J. Lippard, *J. Am. Chem. Soc.* **2003**, *125*, 14082–14092.
[52] Y. Mantri, S. J. Lippard, M.-H. Baik, *J. Am. Chem. Soc.* **2007**, *129*, 5023–5030.
[53] P. M. Pil, S. J. Lippard, *Science*, **1992**, *256*, 234–237.
[54] F. J. Dijt, J.-C. Chottard, J.-P. Girault, J. Reedijk, *Eur. J. Biochem.* **1989**, *179*, 333–344.
[55] K. Inagaki, Y. Kidani *Inorg. Chim. Acta* **1983**, *80*, 171–176.
[56] S. Teletchéa, S. Komeda, J.-M. Teuben, M.-A. Elizondo-Riojas, J. Reedijk, J. Kozelka, *Chem. Eur. J.* **2006**, *12*, 3741–3753.
[57] G. Admiraal, M. Alink, C. Altona, F. J. Dijt, C. J. van Garderen, R. A. G. de Graaff, J. Reedijk, *J. Am. Chem. Soc.* **1992**, *114*, 930–938.
[58] M. Carlone, L. G. Marzilli, G. Natile, *Eur. J. Inorg. Chem.* **2005**, 1264–1273.
[59] N. Hadjiliadis, T. Theophanides, *Inorg. Chim. Acta*, **1975**, *15*, 167–178.
[60] F. J. Dijt, G. W. Canters, J. H. J. den Hartog, A. T. M. Marcelis, J. Reedijk, *J. Am. Chem. Soc.* **1984**, *106*, 3644–3647.
[61] It has been demonstrated, however, that the pK_a values of neutral acids (and their conjugated bases) increase in organic solvents as compared to water (the decrease in the dielectric constant of the medium disfavors dissociation of neutral acids because it produces charged species, thus it increases the pK_a values;[62] for example., the pK_a value of acetic acid is 4.76 and 22.3 in H_2O and CH_3CN, respectively.[63]
[62] M. Rosés, *J. Chromatography A* **2004**, *1037*, 283–298.
[63] S. Espinosa, E. Bosch, M. Rosés, *J. Chromatography A* **2002**, *964*, 55–66.
[64] L. C. Sowers, G. V. Fazakerley, H. Kim, L. Dalton, M. F. Goodman, *Biochemistry* **1986**, *25*, 3983–3988.
[65] R. Fernández, M. Melchart, A. Habtemariam, S. Parsons, P. J. Sadler, *Chem. Eur. J.* **2004**, *10*, 5173–5179.
[66] E. Y. Bivián-Castro, M. Roitzsch, D. Gupta, B. Lippert, *Inorg. Chim. Acta* **2005**, *358*, 2395–2402.
[67] A. F. A. Peacock, S. Parsons, P. Sadler, *J. Am. Chem. Soc.* **2007**, *129*, 3348–3357.
[68] J. L. van der Veer, H. van den Elst, J. H. J. den Hartog, A. M. J. Fichtinger-Schepman, J. Reedijk, *Inorg. Chem.* **1986**, *25*, 4657–4663.
[69] R. Stuart, M. G. Harris, *Can. J. Chem.* **1977**, *55*, 3807–3814.
[70] F. Zamora, M. Kunsman, M. Sabat, B. Lippert, *Inorg. Chem.* **1997**, *36*, 1583–1587.
[71] G. Kampf, L. E. Kapinos, R. Griesser, B. Lippert, H. Sigel, *J. Chem. Soc. Perkin Trans. 1* **2002**, 1320–1327.
[72] V. Reichelová, F. Albertioni, J. Liliemark, *J. Chromatography A* **1994**, *667*, 37–45.
[73] I. Velikyan, S. Acharya, A. Trifonova, A. Foldesi, J. Chattopadhyaya, *J. Am. Chem. Soc.* **2001**, *123*, 2893–2894.
[74] J. Kasparkova, K. J. Mellish, Y. Qu, V. Brabec, N. Farrell, *Biochemistry* **1996**, *35*, 16705–16713.
[75] L. J. Rinkel, C. Altona, *J. Biomol. Struct. Dyn.* **1987**, *5*, 621–649.
[76] As expected, the 3′-A N1H and 5′-A N1H resonances of $[Rh_2(DTolF)_2\{d(GpA)\}]$ and $[Rh_2(DTolF)_2\{d(ApG)\}]$, respectively, are not detected in protic solvents; they appear as sharp ^{1}H NMR signals in CD_3CN at temperatures below −20 °C and split into doublets at −38 °C. Their absence from the spectra at room temperature and the broadness of these resonances at temperatures above −20 °C results from their fast exchange (on the NMR time scale) with residual water present in CD_3CN. At −38 °C in CD_3CN, both adenine N1H resonances appear as doublets at $\delta = 10.32$ ppm (3′-A) and $\delta = 7.29$ ppm (5′-A) for $[Rh_2(DTolF)_2\{d(GpA)\}]$ and $[Rh_2(DTolF)_2\{d(ApG)\}]$, respectively, owing to slower exchange of the N1H protons with residual water at low temperatures. The exchange of the N1H protons with residual water is also confirmed by the exchange spectroscopy (EXSY) cross-peaks between residual water in CD_3CN and the adenine N1H resonances.
[77] D. G. Gorenstein in *Phosphorus-31 NMR*; (Ed.: D. G. Gorenstein), Academic, New York, **1984**.

[78] L. G. Marzilli, P. A. Marzilli, E. Alessio, *Pure Appl. Chem.* **1998**, *70*, 961–968.
[79] The degree and direction of the base canting depends on the carrier ligands, the presence of a tether between the bases, the sugar (deoxyribose or ribose), the presence of a 5′ flanking residue as well as the single- or double-stranded nature of the DNA.[37]
[80] F. P. Intini, R. Cini, G. Tamasi, M. B. Hursthouse, G. Natile, *Inorg. Chem.* **2008**, *47*, 4909–4917.
[81] A. Anagnostopoulou, E. Moldrheim, N. Katsaros, E. Sletten, *J. Biol. Inorg. Chem.* **1999**, *4*, 199–208.
[82] J. Raber, C. Zhu, L. A. Eriksson, *J. Phys. Chem. B* **2005**, *109*, 11006–11015.
[83] J. H. J. den Hartog, C. Altona, J. C. Chottard, J. P. Girault, J. Y. Lallemand, F. A. A. M. de Leeuw, A. T. M. Marcelis, J. Reedijk, *Nucleic Acids Res.* **1982**, *10*, 4715–4730.
[84] B. Lippert, H. Schöllhorn, U. Thewalt, *Inorg. Chim. Acta* **1992**, *198–200*, 723–732.
[85] M. D. Topal, J. R. Fresco, *Nature* **1976**, *263*, 285–289.
[86] W. Saenger, *Principles of Nucleic Acid Structure*, Springer, Berlin **1984**, p. 61.
[87] F. Delaglio, S. Grzesiek, G. W. Vuister, G. Zhu, J. Pfeifer, A. Bax, *J. Biomol. NMR* **1995**, *6*, 277–293.
[88] S. Espinosa, E. Bosch, M. Rosés, *Anal. Chem.* **2000**, *72*, 5193–5200.
[89] T. Mussini, A. K. Covington, P. Longhi, S. Rondinini, *Annali di Chim.* **1983**, *73*, 675–683.
[90] A. K. Rappé, C. J. Casewit, K. S. Colwell, W. A. Goddard III, W. M. Skiff, *J. Am. Chem. Soc.* **1992**, *114*, 10024–10035.
[91] L. A. Castonguay, A. K. Rappé, *J. Am. Chem. Soc.* **1992**, *114*, 5832–5842.
[92] A. K. Rappé, K. S. Colwell, C. J. Casewit, *Inorg. Chem.* **1993**, *32*, 3438–3450.

Received: June 10, 2008
Published online: October 8, 2008

